Supporting Information

O, N Co-doped 3D graphene Hollow Sphere Derived from Metal-Organic Frameworks as Oxygen Reduction Reaction Electrocatalysts for Zn-air batteries

Ruili Song,[a†] Xiaoting Cao [a†], Jiang Xu[b], Xiaoshuang Zhou[b], Xi Wang[a], Ningyi Yuan[*,a], Jianning Ding[*,a,b]

a. Jiangsu Collaborative Innovation Center for Photovoltaic Science and Engineering, Jiangsu Province Cultivation Base for State Key Laboratory of Photovoltaic Science and Technology, Changzhou University, Changzhou University, Changzhou 213164, P. R. China.

b. Institute of Intelligent Flexible Mechatronics, Jiangsu University, Zhenjiang, 212013, China

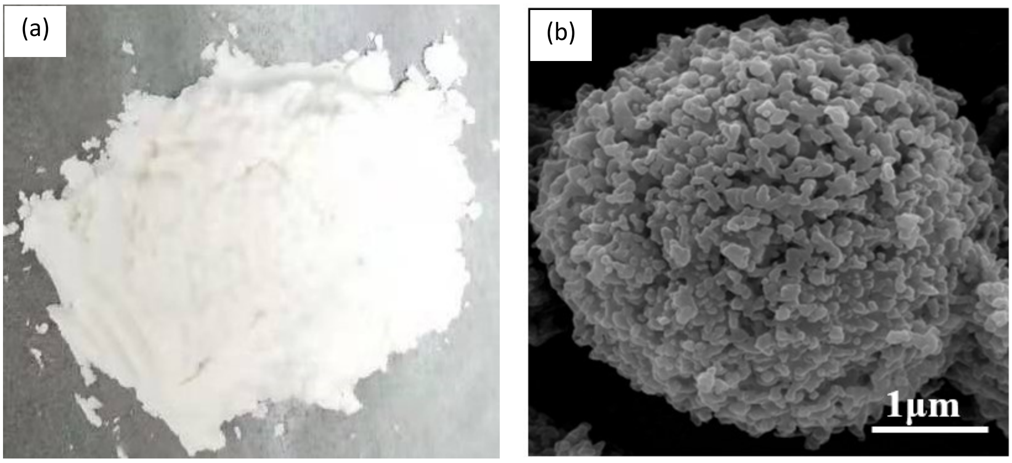

Figure S1. (a) Optical photo of Zn-BTC. (b) FESEM of Zn-BTC.

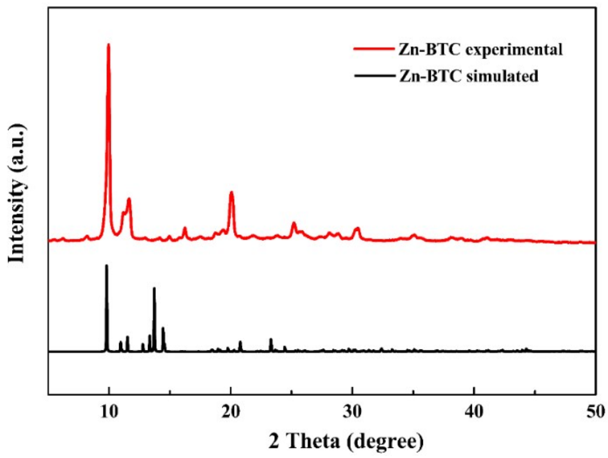

Figure S2. XRD pattern of Zn-BTC

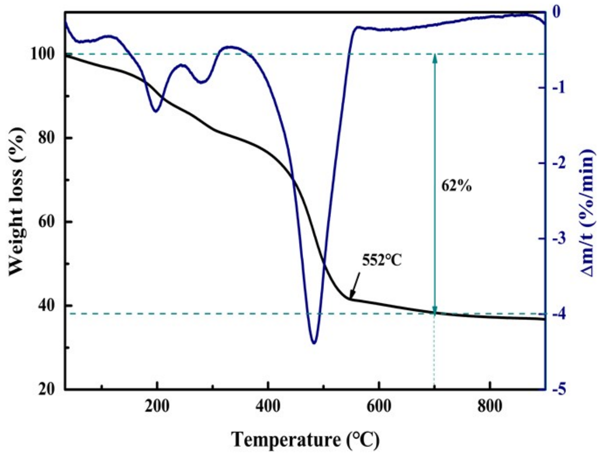

Figure S3. TGA curve of Zn-BTC precursor under nitrogen atmosphere.

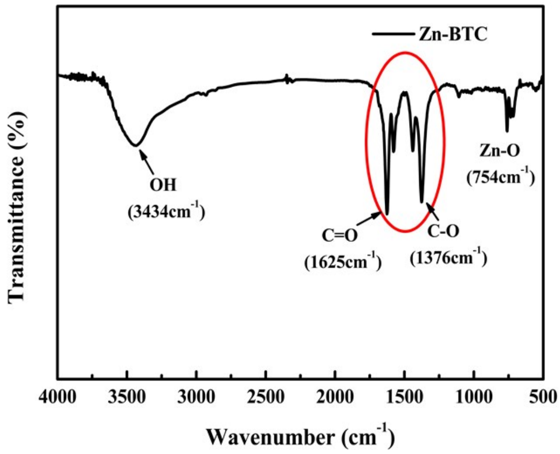

Figure S4. FTIR pattern of Zn-BTC precursor

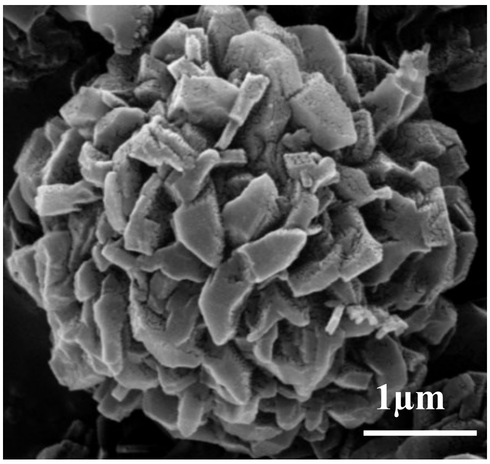

Figure S5. (a) FESEM of ZnO/C.

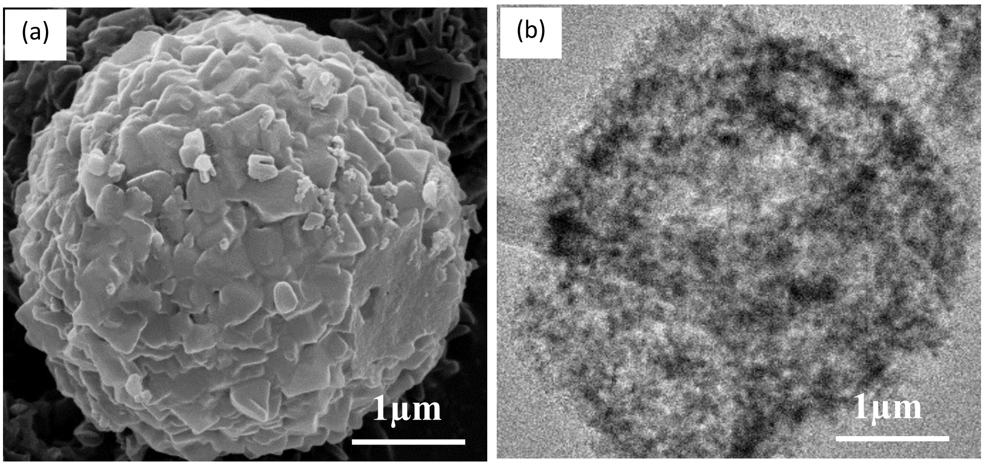

Figure S6. (a) FESEM of ZnO/C-HCl. (b) HRTEM of ZnO/C-HCl.

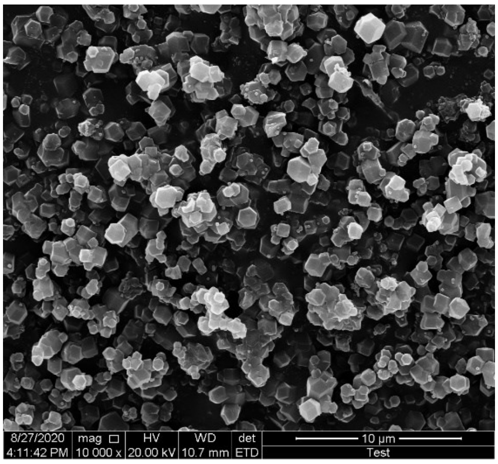

Figure S7. (a) FESEM of N-graphene.

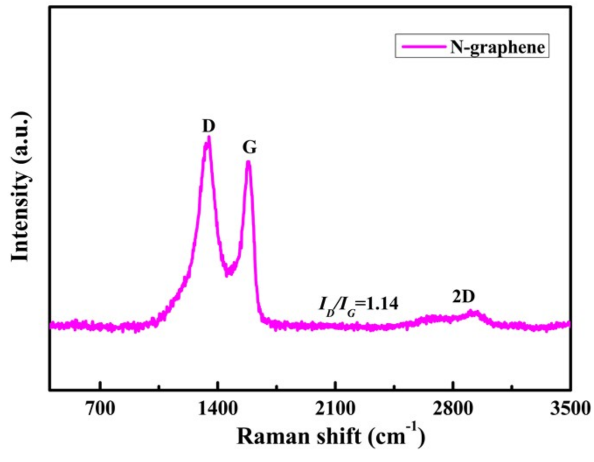

Figure S8. Raman spectra of N-graphene.

Table S1. BET surface areas and pore volumes of the N-graphene, ZnO/C, ZnO/C-HCl, and O, N-graphene

Sample	BET surface area (m^2g^{-1})	$V_{micropore}$/ $V_{micropore+mesopore}$	$V_{mesopore}$/ $V_{micropore+mesopore}$	Total pore volume (cm^3g^{-1})	Pore size (nm)
N-graphene	697.6	19%	81%	0.394	2.26
ZnO/C	1577.44	30%	70%	1.01	2.50
ZnO/C-HCl	1621.58	21%	79%	1.11	2.81
O, N-graphene	1801.45	21.6%	78.4%	1.43	3.18

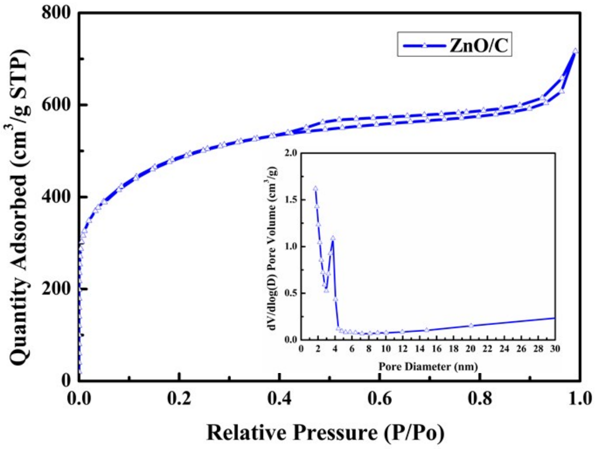

Figure S9. Nitrogen adsorption-desorption isotherm of ZnO/C, and inset shows the corresponding pore size distribution of ZnO/C.

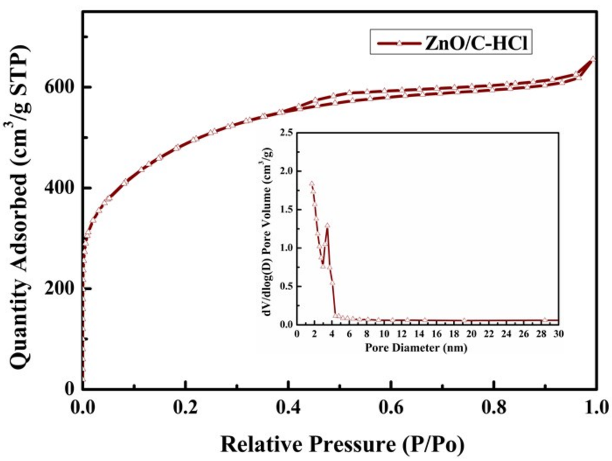

Figure S10. Nitrogen adsorption-desorption isotherm of ZnO/C-HCl, and inset shows the corresponding pore size distribution of ZnO/C-HCl.

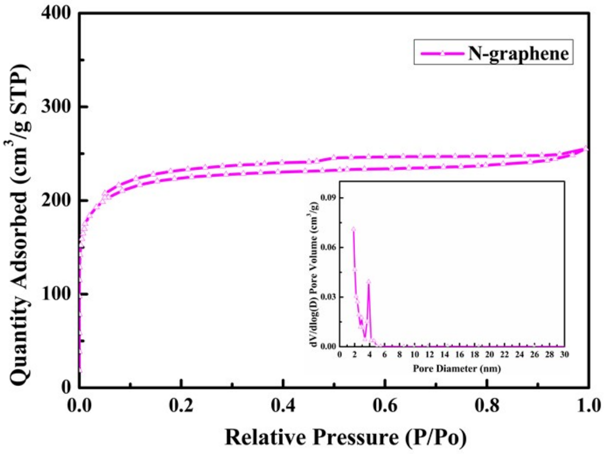

Figure S11. Nitrogen adsorption-desorption isotherm of N-graphene, and inset shows the corresponding pore size distribution of N-graphene.

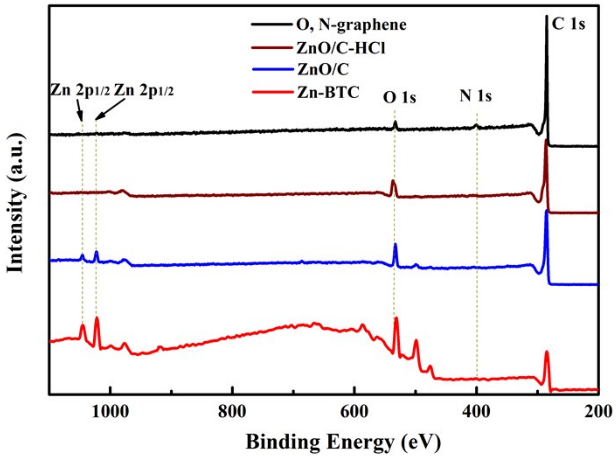

Figure S12. XPS survey spectra for Zn-BTC, ZnO/C, ZnO/C-HCl, and O, N-graphene.

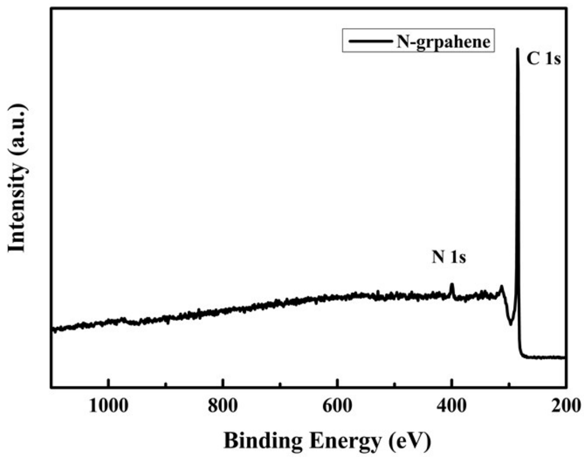

Figure S13. XPS survey spectra of N-graphene.

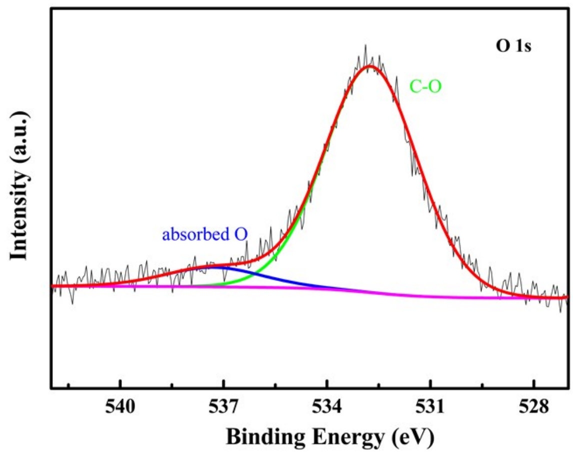

Figure S14. O 1s XPS spectra of O, N-graphene.

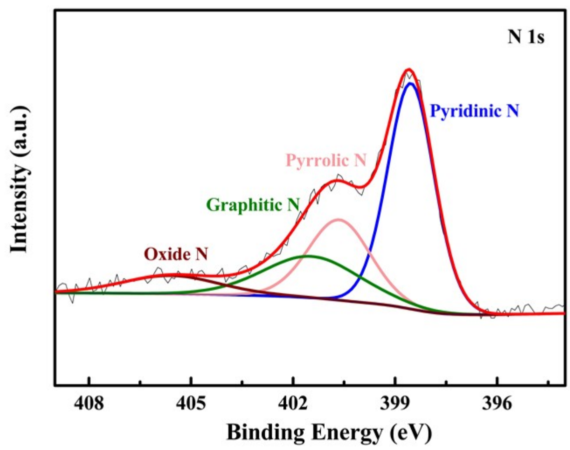

Figure S15. N 1s XPS spectra of N-graphene.

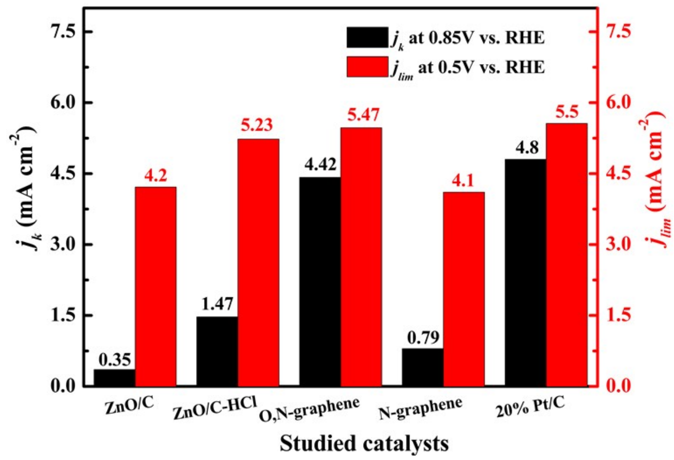

Figure S16. Onset potential and half-wave potential of ZnO/C, ZnO/C-HCl, O, N-graphene, N-graphene, and 20wt% Pt/C.

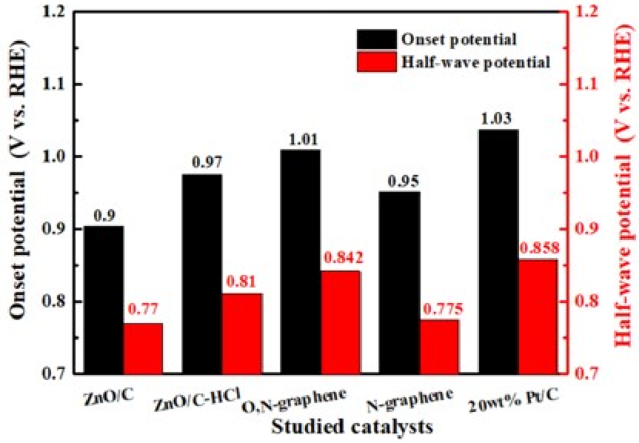

Figure S17. Kinetic current density at 0.85 V *vs.* RHE and limiting current density at 0.5 V *vs.* RHE of ZnO/C, ZnO/C-HCl, O, N-graphene, N-graphene, and 20wt% Pt/C.

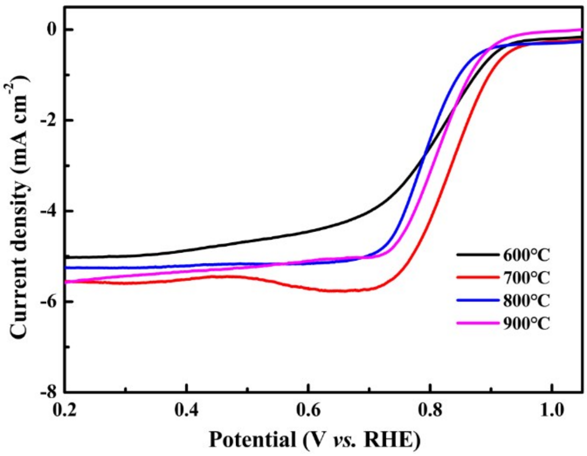

Figure S18. LSV curves of O, N-graphene pyrolyzed at different temperatures at 10 mV s^{-1}.

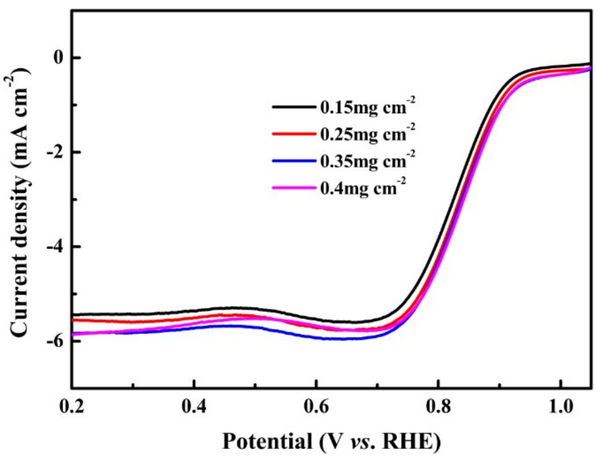

Figure S19. LSV curves of O, N-graphene under different loads at 10 mV s^{-1} and a rotating speed of 1600 rpm.

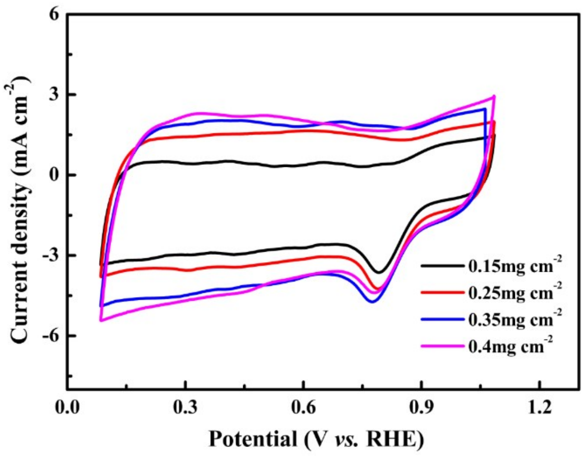

Figure S20. CV curves of O, N-graphene under different loads at 50 mV/s.

Table S2. Comparison of electrocatalytic activities of O, N-graphene with the state-of-the-art catalysts

Items	Catalyst	Dopped elements	Onset potential	Half-wave potential	Diffusion-limited Current density	Loading (0.1 M KOH)	Reference
1	**O, N-graphene**	O, N	1.01 vs. RHE	0.842 vs. RHE	5.47 mA cm^{-2}	0.25	This work
2	**NOGB-800**	N, O	0.92 vs. RHE	0.84 vs. RHE	5.5 mA cm^{-2}	0.4	1
3	**BNPC-1100**	N, P	0.894 vs. RHE	0.803 vs. RHE	4.73 mA cm^{-2}	0.4	2
5	**N, S-CN**	N, S	0.92 vs. RHE	0.77 vs. RHE	5.35 mA cm^{-2}	0.2	3
6	**N-doped graphene**	N	0.95 vs. RHE	-	-	0.2	4
7	**GH-BGQD**	B	0.93 vs. RHE	-	5.74 mA cm^{-2}	-	5
8	**N-graphene/CNT**	N	0.98 vs. RHE	0.69 vs. RHE	-	0.2	6
9	**BCN Graphene**	B, N	-	-0.25 V vs. SCE	-	-	7
10	**PG**	P	0.92 vs. RHE	-	-	0.051	8
11	**N-RGO-800**	N	0.876 vs. RHE	0.725 vs. RHE	5.21 mA cm^{-2}	-	9
12	**S_1N_6C-900**	N, S	0.95 vs. RHE	0.83 vs. RHE	4.86 mA cm^{-2}	-	10
13	**N-GA-150**	N	-	0.77 vs. RHE	-	0.102	11

1 Q. Hu, G. Li, G. Li, X. Liu, B. Zhu, X. Chai, Q. Zhang, J. Liu, C. He, *Advanced Energy Materials*, 2019, **9**(14), 1803867.

2 J. Zhang, Z. Zhao, Z. Xia, L. Dai, *Nature Nanotechnology*, 2015, 10, 444-452.

3 K. Qu, Y. Zheng, S. Dai, S. Z. Qiao, Nano Energy, 2016, 19, 373-381.

4 H. Cui, M. Jiao, Y. Chen, Y. Guo, L. Yang, Z. Xie, Z. Zhou, S. Guo, *Small Methods*, 2018, **2**(10), 1800144.

5 T. V. Tam, S. G. Kang, M. H. Kim, S. G. Lee, S. H. Hur, J. S. Chung, W. M. Choi, *Advanced Energy Materials*, 2019, **9** (26), 1900945.

6 Z. Wen, S. Ci, Y. Hou, J. Chen, *Angew. Chem. Int. Ed.*, 2014, **53**, 6496-6500.

7 S. Wang, L. Zhang, Z. Xia, A. Roy, D. W. Chang, J. B. Baek, L. Dai, *Angewandte Chemie International Edition*, 2012, **51**(17), 4209-4212.

8 C. Zhang, N. Mahmood, H. Yin, F. Liu, Y. Hou, *Advanced materials*, 2013,**25**(35), 4932-4937.

9 H. Miao, S. Li, Z. Wang, S. Sun, M. Kuang, Z. Liu, J. Yuan, International Journal of Hydrogen Energy, 2017, **42**(47), 28298-28308.

10 J. Li, Y. Zhang, X. Zhang, J. Huang, J. Han, Z. Zhang, X. Han, P. Xu, B. Song, *ACS applied materials & interfaces*, 2017, **9**(1), 398-405.

11 Q. Xue, Y. Ding, Y. Xue, F. Li, P. Chen, Y. Chen, *Carbon*, 2018, **139**, 137-144.